


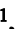



Biologically Active Polyethylene Glycol-Based Multiple-Catechol-Containing Biopolymer Poly[3-(3,4-dihydroxyphenyl)glyceric acid] from Different Medicinal Plants of Boraginaceae Family

Vakhtang Barbakadze ^{1, *} , Maia Merlani ^{1, }, Lali Gogilashvili ^{1, }, Lela Amiranashvili ^{1, }, Karen Mulkijanyan ^{2, }

V.B. – Research Scientist, v.barbakadze@tsmu.edu, tel. 595 53 15 09

M.M. – Head of the Department, Principal Research Scientist, m.merlani@tsmu.edu, tel. 599 761 117

L.G. – Senior Research Scientist, l.gogilashvili@tsmu.edu, tel. 599 347 042

L.A. – Senior Research Scientist, l.amiranashvili@tsmu.edu, tel. 577 723 144

K.M. – Head of the Department, Principal Research Scientist. k.mulkijanyan@tsmu.edu, 555 235 829

¹Department of Plant Biopolymers and Chemical Modification of Natural Compounds, Tbilisi State Medical University, I.Kutateladze Institute of Pharmacochimistry, Tbilisi 0159, Georgia

²Department of Preclinical Pharmacological Research, Tbilisi State Medical University, I.Kutateladze Institute of Pharmacochimistry, Tbilisi 0159, Georgia

*Correspondence v.barbakadze@tsmu.edu

Abstract

High molecular weight (>1000 kDa or >500 kDa) water-soluble preparations (HMPs) from *Symphytum asperum*, *S. caucasicum*, *S. officinale*, *S. grandiflorum*, *Anchusa italica*, *Cynoglossum officinale*, *Borago officinalis*, and *Paracynoglossum imeretinum* (Boraginaceae) were obtained. The main chemical constituent of these HMPs is the first and only representative of a previously unreported class of natural polyethers — a novel poly[oxy-1-carboxy-2-(3,4-dihydroxyphenyl)ethylene], also known as poly[3-(3,4-dihydroxyphenyl)glyceric acid] (P-DGA). The structure elucidation of P-DGA was performed using data from various nuclear magnetic resonance (NMR) techniques, including liquid-state ¹H, ¹³C NMR, two-dimensional (2D) homonuclear gCOSY, two-dimensional (2D) heteronuclear ¹H/¹³C gHSQCED, two-dimensional (2D) DOSY (Diffusion-ordered spectroscopy), and solid-state ¹³C NMR spectra. The polyoxyethylene (polyethylene glycol) (PEG) chain serves as the backbone of this biopolymer, with a residue of 3-(3,4-dihydroxyphenyl)glyceric acid functioning as the repeating unit. The 3,4-dihydroxyphenyl (catechol) and carboxyl groups consistently substitute for two carbon atoms in the PEG backbone chain. Hence, P-DGA represents a unique class of natural polyethers. Each repeating trifunctional structural unit of P-DGA contains two phenolic hydroxyl groups in the ortho position and one carboxyl group. The multifunctionality of P-DGA likely explains its wide spectrum of biological activities, including anti-complementary, antioxidant, anti-inflammatory, burn and wound healing, antimicrobial, and anti-cancer properties.

Keywords: natural polyethers; poly[3-(3,4-dihydroxyphenyl)glyceric acid]; Boraginaceae; catechol; polyethylene glycol.

1. Introduction

Herbs can be seen as biosynthetic chemical laboratories that produce numerous chemical compounds. Chemicals with medicinal benefits are known as “active ingredients” or “active principles.” Plant-derived products, also referred to as herbal or phytotherapeutic products, demonstrate a broad therapeutic spectrum. The bioactive constituents of herbal products, such as alkaloids, flavonoids, terpenes, and polyphenols, can interact with biological systems, leading to the discovery of novel drugs that provide therapeutic benefits [1-4]. Plants used in traditional medicine have endured the test of time. Medicinal plant extracts can contain hundreds or thousands of bioactive compounds in varying abundances, making it a significant challenge to identify the compounds responsible for specific biological activities [5].

Phytochemicals are categorized into primary and secondary metabolites based on their roles in plant metabolism. Primary metabolites essential for plant survival include carbohydrates, amino acids, proteins, lipids, purines, and pyrimidines found in nucleic acids. In contrast, secondary metabolites consist of other chemical compounds produced from metabolic pathways that diverge from the primary metabolic routes [6]. A wide variety of secondary metabolites intrigues scientists, particularly due to their unique pharmacophores and medicinal properties.

Polymers of natural origin are known as “biopolymers”—macromolecules typically produced by living systems, including plants, animals, and microorganisms. In recent years, there has been a growing trend toward the use of more biopolymers in the development of various food and medical products [7, 8]. Compared to synthetic polymers, biopolymers offer several advantages, such as biocompatibility, biodegradability, abundant renewable sources, and the ability to metabolize in the human body without releasing toxic or harmful products [8, 9]. The United States Food and Drug Administration (US FDA) has approved many biopolymer-based products. Biopolymers are made up of repeating units of monomers, such as sugars, amino acids, or fermentative products like aliphatic polyesters. These biopolymers may possess different functional groups: hydroxyl, amino, amide, carboxyl, phosphate, and phenolic, which impart various biological activities. Biopolymers are generally classified into three groups: polysaccharides, proteins, and polynucleotides [7, 8].

Another significant group of plant-derived compounds is phenolics, which provide numerous beneficial effects on human health due to their antioxidant, anti-inflammatory, antithrombotic, antiallergenic, anticancer, antifungal, antimicrobial, and antiatherosclerosis properties [10]. Phenolic compounds are widespread secondary metabolites produced in plants through the shikimate, pentose phosphate, and phenylpropanoid pathways [10, 11]. They consist of hydroxybenzenes that contain an aromatic ring with one or more hydroxyl substituents. These compounds can be divided into two main groups: simple phenols and polyphenols, based on the number of phenol units in their structure [10-12]. The antioxidant activity, the most notable property of phenolic compounds, relates to their structure, specifically the number and position of hydroxyl groups in relation to carboxyl groups [10]. Various mechanisms have been described regarding the effects of phenolic compounds on health: they

reduce the expression of inflammatory factors, increase brain-derived neurotrophic factor expression, modulate the gut microbiota, decrease cancer cell proliferation, and enhance apoptosis induction [10, 12]. Plant phenols range from simple phenolic molecules to highly polymerized compounds. Phenolic phytochemicals are also classified into two main categories: (i) water-soluble (e.g., phenolic acids, hydrolyzable tannins (ellagitannin), phenylpropanoids, flavonoids, and quinones) and (ii) water-insoluble (e.g., condensed tannins, lignins, and cell wall-bound hydroxycinnamic acids) [12]. The covalent conjugation of phenolics with other biomolecules (proteins, polysaccharides, fatty acids, etc.) and electrostatic interactions with metal ions (silver, gold, iron, zinc, etc.) enhance their functionality and applications [12].

Among a wide variety of phenolics, catechol (*ortho*-dihydroxybenzene) derivatives and their corresponding *ortho*-quinones represent an important class that is widespread in many living organisms, including mussels, sandcastle worms, geckos, insects, and squids. They play a crucial role in numerous biological processes and functions. Due to their unique chemical and physico-chemical properties, the remarkable biological activity of catechols encourages scientists to develop countless advanced multifunctional materials with outstanding and fascinating properties through the synergistic combination of catechols and polymers [13].

Among the catechol-containing natural products that have attracted considerable attention for their diverse biological activities and low toxicity are hydroxycinnamic acid derivatives, such as caffeic acid [14].

The Boraginaceae family includes approximately 2000 species worldwide, mainly in Europe and Asia. The therapeutic effects of these plants are attributed to the presence of various biologically active compounds, such as naphthoquinones, flavonoids, terpenoids, and phenols, which display antimicrobial, antitumor, antiviral, anti-inflammatory, cardiogenic, contraceptive, and antiplatelet activities. However, these plants are also high in hepatotoxic pyrrolizidine alkaloids, which significantly restrict their use. Nevertheless, applying Boraginaceae plants as a poultice for wounds remains acceptable. Despite the beneficial qualities of Boraginaceae plants, their medical application is still controversial [15-17].

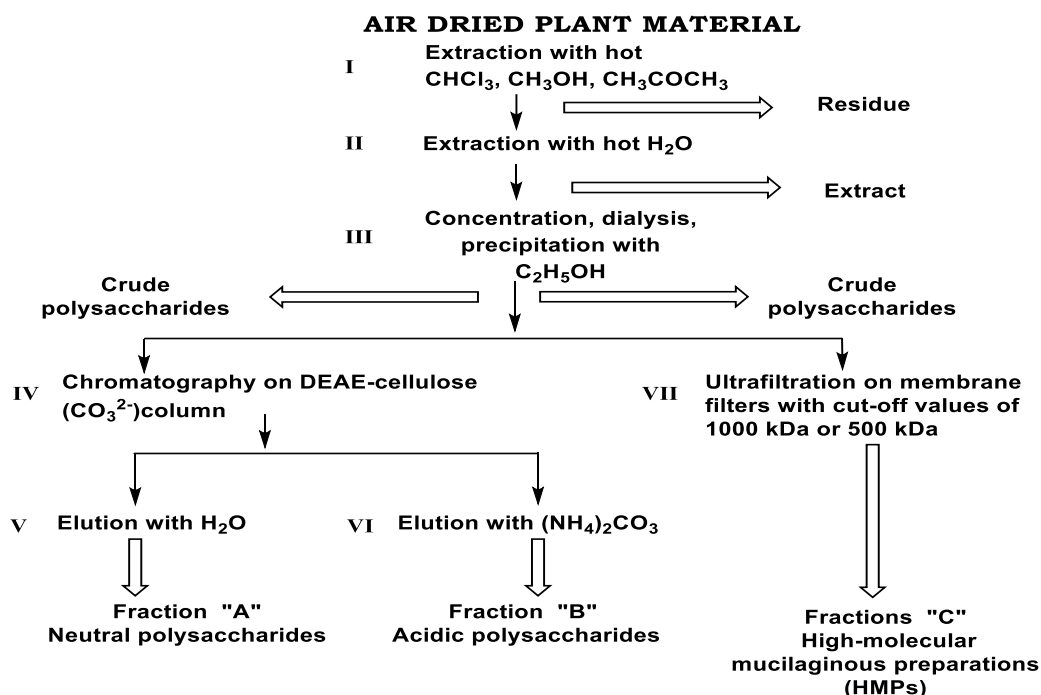
Ether bonds are found in a wide variety of natural products, mainly secondary metabolites, including lipids, oxiranes, terpenoids, flavonoids, polyketides, and carbohydrate derivatives or aromatic polymers such as lignin [18]. In the latter case, peroxidases initiate the radical coupling of monolignols to lignin, yielding ether links between two aromatic rings or between an aromatic ring and an aliphatic moiety [19]. However, reports concerning biopolymers containing aliphatic ethers as repeating units are sparse. Within the field of pharmacologically active biopolymers, the area of stable natural polyethers seems relatively new and rather attractive.

This review aims to consolidate knowledge about the isolation, fractionation, detection, and structural elucidation of the first representative of a unique class of natural polyethers, which exhibits a broad spectrum of biological activity. This activity originates from the routine assessment results of the anticomplementary and antioxidant activities of crude polysaccharides isolated from *S. aspeum* and *S. caucasicum*.

2. Materials and Methods

2.1. Bioactivity-guided Isolation of the Main Chemical Constituent of Water-soluble High-molecular Preparations (HMPs) from Various Genera and Species of the Boraginaceae Family

Medicinal plants, including *Symphytum asperum* (SA), *S. caucasicum* (SC), *S. officinale* (SO), *S. grandiflorum* (SG), *Anchusa italica* (AI), *Cynoglossum officinale* (CO), *Borago officinalis* (BO), and *Paracynoglossum imeretinum* (PI) (Boraginaceae), are widely distributed across the Caucasus, particularly in Georgia. The raw plant materials — roots or stems — were cut into small pieces, air-dried, and ground. Lipids, pigments, and low-molecular-weight compounds (monosaccharides, phenolics, etc.) were extracted using Soxhlet extraction with chloroform, methanol, and acetone. The hot-water extraction of the pretreated materials was followed by dialysis, resulting in crude water-soluble polysaccharides with immunomodulatory activity, including anticomplementary and antioxidant activities [20]. A general strategy involving the fractionation of bioactive crude water-soluble polysaccharides and the isolation of active principles was used to identify new or novel compounds responsible for that activity, utilizing both i) bioactivity-guided and ii) structure-directing isolation [21]. Consequently, the fractionation of crude polysaccharides was carried out using molecular mass-based ultrafiltration (UF) under a nitrogen pressure of 3 atmospheres in a stirred ultrafiltration cell. Various membranes with cut-off values of 10 kDa, 100 kDa, 500 kDa, and 1000 kDa were employed. During the UF process, the fractionation was monitored by evaluating anticomplementary and antioxidant activities and measuring total sugars and UV absorption at 286 nm in both the solutions and effluents. Fractions containing molecules with relative molecular masses (M_r) above 1000 kDa or 500 kDa exhibited higher anticomplementary and antioxidant activities than crude polysaccharides. These active fractions had low carbohydrate content and showed strong UV absorption at 286 nm, unlike high carbohydrate content fractions below 500 kDa, which exhibited neither anticomplementary nor antioxidant activity. Thus, the removal of most ballast bio-inactive polysaccharides and the acquisition of water-soluble high-molecular-weight preparations (HMPs) greater than 1000 or 500 kDa has been facilitated by UF (**Scheme 1, fraction “C”**) [20, 22]. In addition, the UF enabled the complete removal of hepatotoxic and carcinogenic pyrrolizidine alkaloids with an average weight of 340 Da, characteristic of Boraginaceae family species [23].



Scheme 1. Isolation of **HMPs** from **SA**, **SC**, **SO**, **SG**, **AI**, **CO**, **BO**, and **PI**.

Fractions "A" and "B" represent neutral glucofructan and pectin-type acidic arabinogalactan, respectively [24].

HMPs with a low carbohydrate concentration (approx. 20%) and strong UV absorption at 286 nm displayed significant anti-complementary activity and antioxidant properties. However, sugars do not absorb light in the typical UV range due to their lack of chromophores. The monosaccharide composition of **HMPs** notably differed from that of the initial crude polysaccharide extracts. **HMPs** included rhamnose, arabinose, mannose, glucose, galactose, uronic acids, and minimal amounts of fructose. Subsequently, **HMPs** underwent gel chromatography on a Sepharose 2B column. Equal volumes of eluents were examined for the inhibition of human complement activity, total sugar content, and UV absorption at 286 nm. The elution profile showed anti-complementary activity that coincided with a UV absorption pattern at 286 nm but did not correspond with the carbohydrate elution.

To characterize an immunomodulatory component of **HMPs**, it was treated with skin powder. The modulatory effect on human complement significantly decreased, while also reducing absorption in the UV range. The absorption of active substances by skin powder, along with the UV spectrum of these compounds, exhibited an absorption maximum at 286 nm, attributable to phenolic substances, which suggested the presence of a phenolic moiety in the structure of the active compounds. Based on this data, we hypothesized that the isolated bioactive compounds are phenolic polymers, and their presence in crude polysaccharides can be explained by their similar hydrophilicity [20].

2.2. The Elucidation of the Structure of the Main Chemical Constituent of HMPs from Various Genera and Species within the Boraginaceae Family

The elucidation of the structure of a main chemical constituent of HMPs from SA, SC, SO, SG, AI, CO, BO, and PI was based on data obtained from UV, IR, and various NMR spectroscopy techniques in both liquid and solid states (Figs. 1-14, Tables 1-5).

The absorption maxima observed in the UV spectrum of HMPs from SA, SC, SO, SG, AI, CO, BO, and PI were found at 212 nm, 236 nm (shoulder), 282 nm (shoulder), and 286 nm (H₂O, λ_{max} , nm), which can be attributed to substituted phenols. Typically, catechol exhibits an absorbance peak of around 270–290 nm [25].

The IR spectra of HMPs from SA, SC, SO, SG, AI, CO, BO, and PI were recorded using KBr (KBr, ν , cm⁻¹). They exhibited bands at 3425 (OH), 2924 (CH), 1605 (ionized carboxyl), 1512 and 1443 (aromatic C=C), 1404 and 1219 (phenols), 1265, 1080, and 1018 (R-O-R'), 872 (C-H in the aromatic ring with one isolated hydrogen atom), and 818 cm⁻¹ (C-H in the aromatic ring with two neighboring hydrogen atoms) [26]. The spectrum contains absorption bands characteristic of phenol-carboxylic acids.

The elucidation of the main chemical constituents of HMPs from SA, SC, SO, CO, PI (Figs. 1-6 and 8, Tables 1-3) [27-33] and SG, AI, BO (Figures 9-14, Tables 4 and 5) [34-36] was performed at 80 °C using various techniques in liquid-state and solid-state NMR spectroscopy.

According to the data from the liquid-state ¹³C NMR spectrum (Figure 1) of HMPs derived from SA, SC, SO, CO, and PI, nine distinct signals corresponding to the carbon atoms of the substituted phenylpropionic acid fragment are observed (Figure 4). Interestingly, the signals from the carbohydrate components are nearly unobservable in the HMP spectra (Figure 1), likely due to their diverse monosaccharide composition, which includes rhamnose, arabinose, mannose, glucose, galactose, uronic acids, and only trace amounts of fructose. The broadened signal at 175.4 ppm is assigned to the carboxyl group in the compound.

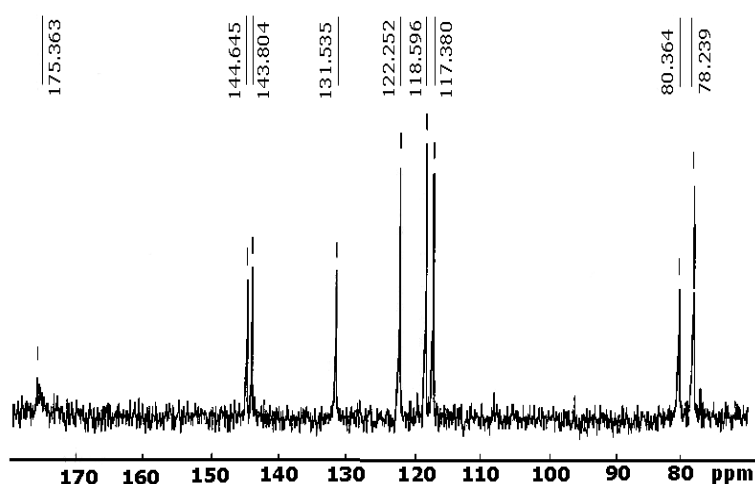


Figure 1. The ¹³C NMR spectrum of HMPs from SA, SC, SO, CO, and PI at 80 °C.

The attached proton test (APT) technique [37] revealed (Figure 2) that five signals are assigned to CH groups and four signals to the non-protonated carbon atoms. The two signals with chemical

shifts of 78.2 and 80.4 ppm correspond to oxygen-bound protonated aliphatic carbon atoms. Six signals were assigned to aromatic carbon atoms (protonated atoms at 117.4, 118.6, and 122.3 ppm and non-protonated atoms at 131.5, 143.8, and 144.7 ppm) (**Figure 2**) [27-29].

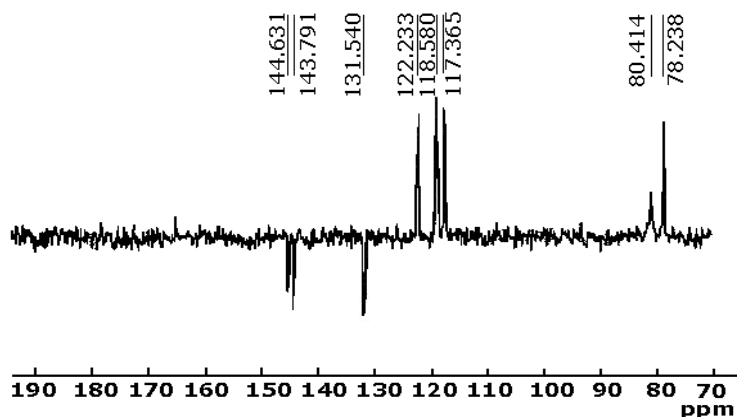


Figure 2. The proton attachment test (APT) spectrum of **HMPs** from **SA**, **SC**, **SO**, **CO**, and **PI** at 80 °C.

The ^1H NMR spectrum of **HMPs** from **SA**, **SC**, **SO**, **CO**, and **PI** displays four signals at 4.9, 5.3, 7.1, and 7.2 ppm, with one of these (7.1 ppm) showing double the intensity (**Figure 3**). Unfortunately, the spin-spin coupling constants could not be determined due to the broadening of these signals.

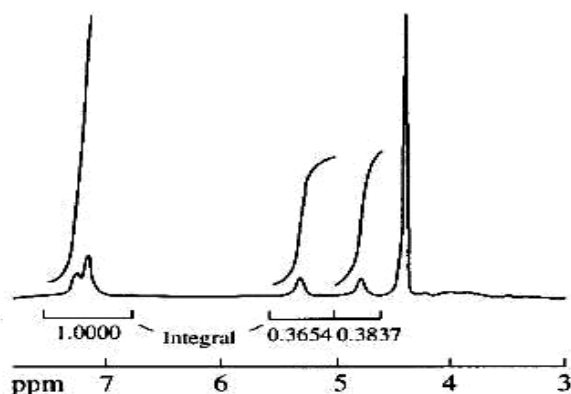


Figure 3. The ^1H NMR spectrum of **HMPs** from **SA**, **SC**, **SO**, **CO**, and **PI** at 80 °C.

The simulated ^{13}C NMR spectrum was calculated using the ACD/CNMR Version 1.1 program (Advanced Chemistry Development Inc., Canada) (**Table 1**, **Figure 4**) [38-40].

Table 1. Chemical shifts of resonances in the ^{13}C NMR spectrum of **HMPs** from **SA** and **SC**.

Experimental	175.4	144.6	143.8	131.5	122.3	118.6	117.4	80.4	78.2
Calculated*	175.1	145.5	145.1	128.8	118.3	115.7	114.4	82.9	77.2

* Calculated values for the 3-(3,4-dihydroxyphenyl)glyceric acid residue of the corresponding polyether are provided for comparison.

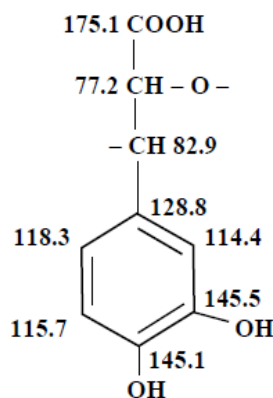


Figure 4. A hypothetical representation of the repeating unit of the biopolymer derived from **SA** and **SC**, which includes the 3-(3,4-dihydroxyphenyl)glyceric acid residue.

The two-dimensional (2D) heteronuclear $^1\text{H}/^{13}\text{C}$ gHSQCED spectrum reveals the following correlations between protons and carbon atoms at 4.9/80.4, 5.3/78.2, 7.1/118.6, 7.1/122.3, and 7.2/117.4 ppm (**Figure 5, Table 2**).

The hydroxyl groups at positions 3 and 4 of the phenyl ring were confirmed by the 1D-NOE experiment conducted in a different mode. Pre-irradiation of the aliphatic proton at position 1 (**Figures 5, 6, and Table 2**), with a chemical shift of 5.3 ppm, provided a NOE for two aromatic protons with chemical shifts of 7.1 (3%) and 7.2 (1%) ppm. Therefore, both *ortho*-positions in the dihydroxyphenyl ring were occupied by protons. The differing NOE values for these two protons, along with their distinct chemical shifts in the ^1H NMR spectrum and the varying positions of resonances of the corresponding carbons in the ^{13}C NMR spectrum, ruled out the possibility of symmetrical bis-meta-substitution of the aromatic ring by two hydroxy groups [27-29].

Based on the data about signal assignments for ^{13}C and ^1H NMR spectra (**Figures 1-4, Table 2**), the correlations observed in the 2D heteronuclear $^1\text{H}/^{13}\text{C}$ gHSQCED (**Figure 5, Table 2**), and in the 2D homonuclear gCOSY (**Figure 6**), the main chemical component of **HMPs** derived from the roots and stems of **SA**, **SC**, **SO**, **CO**, and **PI** is poly[3-(3,4-dihydroxyphenyl)glyceric acid] (**P-DGA**) (**Figure 7A-B**). Consequently, **P-DGA** represents a unique class of multiple-catechol-containing natural polyethers, specifically, poly[oxy-1-carboxy-2-(3,4-dihydroxyphenyl)ethylene], which is also recognized as a caffeic acid-derived biopolymer.

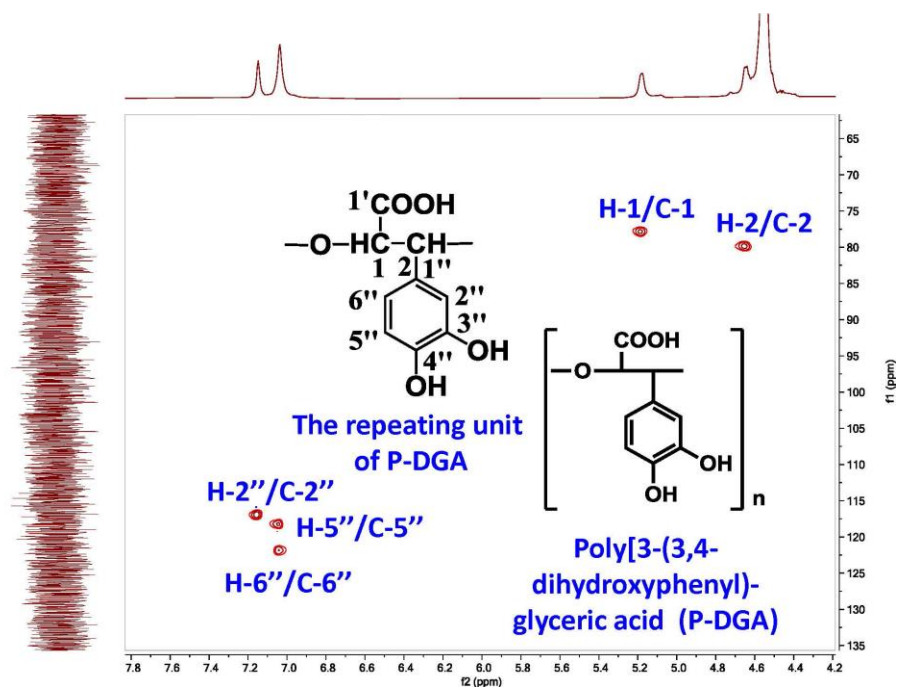


Figure 5. Correlations and assignments of the ^1H and ^{13}C signals in the 2D heteronuclear $^1\text{H}/^{13}\text{C}$ gHSQCED spectrum of **P-DGA** at 80 °C.

The 2D homonuclear gCOSY spectrum (**Figure 6**) showed a cross-peak between the signals at 4.9 and 5.3 ppm, consistent with the coupling between H-1 and H-2 of **P-DGA** (**Figure 6**).

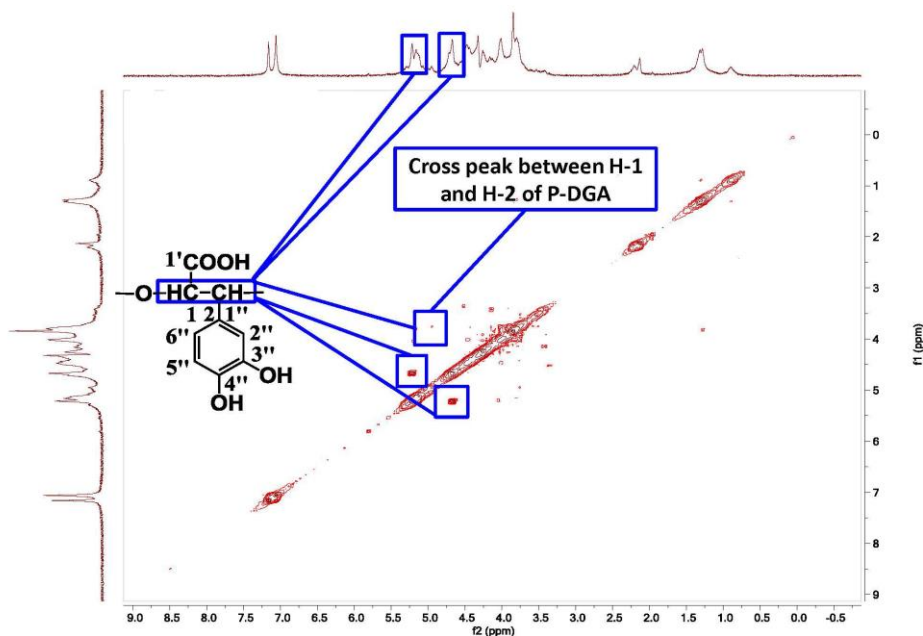
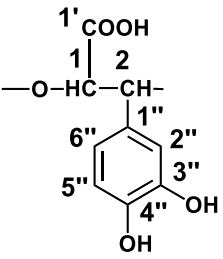


Figure 6. The 2D homonuclear gCOSY spectrum of **P-DGA** at 80 °C.

The total assignment of signals is given in **Table 2**.

Table 2. The signal assignments for the ^{13}C and ^1H NMR spectra of **P-DGA**.

The repeating unit of P-DGA	C atom no.	^{13}C chemical shifts, δ_{C} , ppm	^1H chemical shifts, δ_{H} , ppm
	1'	175.4	
	1	78.2	5.3
	2	80.4	4.9
	1''	131.5	
	2''	117.4	7.2
	3''	144.6	
	4''	143.8	
	5''	118.6	7.1
	6''	122.3	7.1

A good resolution and the narrow shape of the ^{13}C NMR signals indicate that the **P-DGA** is a regular polymer. The polyoxyethylene (polyethylene glycol) (**PEG**) chain serves as the backbone of the polymer molecule. The catechol moieties (3,4-dihydroxyphenyl residues) and carboxyl groups serve as regular substituents on two carbon atoms in the **PEG** backbone chain of **P-DGA** (**Figure 7A**).

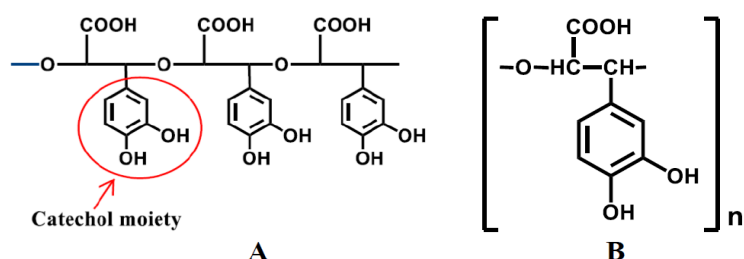


Figure 7. A - Catechol moieties and carboxyl groups are regular substituents at two carbon atoms in the PEG backbone of **P-DGA**; B – Poly[oxy-1-carboxy-2-(3,4-dihydroxyphenyl)ethylene] that is Poly[3-(3,4-dihydroxyphenyl)glyceric acid] (**P-DGA**).

To confirm the proposed structure of the poorly water-soluble high-molecular **P-DGA** from **SA**, the solid-state ^{13}C NMR spectrum was recorded under magic-angle spinning (MAS) conditions. Two different experiments were conducted to assign the ^{13}C signals to the corresponding atoms in the monomer structure. The $^{13}\text{C}\{^1\text{H}\}$ cross-polarization/magic-angle spinning (CP/MAS) NMR experiment is a standard method for spectral assignment of carbon signals. Additionally, a dipolar-dephasing solid-

state NMR pulse sequence with gated decoupling was utilized [41, 42]. The complete assignment of the signals is detailed in **Figure 8** and **Table 3**.

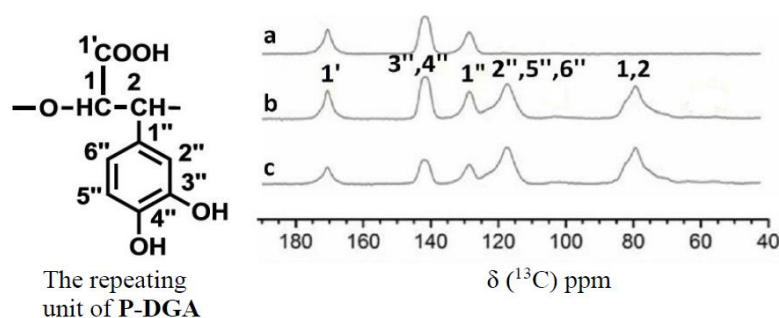


Figure 8. Solid-state $^{13}\text{C}\{^1\text{H}\}$ CP/MAS NMR spectrum of **P-DGA** from **SA**. a) The spectrum was recorded using a 67.0 microseconds (μs) dipolar dephasing filter with a cross-polarization (CP) time of 3.0 milliseconds (ms). b) The spectrum was recorded with a CP time of 3.0 ms. c) The spectrum was recorded with a CP time of 1.0 ms.

Table 3. The assignment of signals in the solid-state $^{13}\text{C}\{^1\text{H}\}$ CP/MAS NMR spectrum of **P-DGA** from **SA** (δ_{C} , ppm).

C atom no.	^{13}C chemical shift, δ_{C} , ppm
1,2	80
1'	174
1''	130
2'', 5'', 6''	118
3'', 4''	143

It is important to emphasize that the resolution of solid-state NMR is inferior to that of liquid-state NMR. For nuclei other than H-1, solid-state NMR peaks are generally at least ten times broader than those of liquid-state NMR. Therefore, the applicability of solid-state NMR spectroscopy to studies is somewhat limited [43]. However, the complete assignment of the signals from the solid-state ^{13}C NMR of **P-DGA** agrees with the results of the liquid-state ^{13}C NMR spectrum (**Figure 1**).

The elucidation of the **P-DGA** structure from **AI**, **SG**, and **BO** was carried out using a similar approach [33-35, 40, 41]. The ^1H NMR, ^{13}C NMR, 2D heteronuclear $^1\text{H}/^{13}\text{C}$ gHSQCED, 2D homonuclear gCOSY, and solid-state ^{13}C NMR spectra of **HMPs** from **AI**, **SG**, and **BO** exhibited a complete set of resonances characteristic of poly[3-(3,4-dihydroxyphenyl)glyceric acid] (**P-DGA**) (**Figures 9-13** and **Tables 4, 5**) [34-36, 41, 42], which are present in the water-soluble high molecular fractions of **SA**, **SC**,

SO, CO, and PI (Figures 1-6, 8 and Tables 1-3) [26-32]. In addition to the aforementioned signals characteristic of the P-DGA from SA, SC, SO, CO, and PI (Figures 1-6, 8 and Tables 1-3) [34-36, 41, 42], the ^{13}C NMR, ^1H NMR, 2D heteronuclear $^1\text{H}/^{13}\text{C}$ gHSQCED, and solid-state ^{13}C NMR spectra of HMPs from AI, SG, and BO displayed the following additional resonances: 54.9 ppm ($-\text{OCH}_3$, ^{13}C NMR, Figure 9); 3.85 ppm ($-\text{OCH}_3$, ^1H NMR, Figure 10); correlation between proton and carbon atoms: 3.85/54.9 ppm ($-\text{OCH}_3$), 2D $^1\text{H}/^{13}\text{C}$ gHSQCED, Figure 11); 54 ppm ($-\text{OCH}_3$, solid-state ^{13}C NMR, Figure 13).

The 2D homonuclear gCOSY spectrum of HMPs from AI, SG, and BO (Figure 12) displayed a cross-peak between the signals at 4.7 and 5.2 ppm, consistent with the coupling between H-1 and H-2 of P-DGA (Figure 12).

The complete signal assignments are presented in Figures 9-13 and Tables 4, 5 [34-36, 41, 42]. The additional signals may be observed in the spectrum of HMPs from AI, SG, and BO due to the presence of the methoxy group. Two non-sharp signals (172.8 and 175.6 ppm, Figure 9) are believed to arise from two carboxyl groups. A resonance in the ^{13}C NMR spectrum at 54.9 ppm, which correlates with the ^1H resonance at 3.85 ppm (Figures 9-12), suggests the presence of methoxy groups are present in carboxylic acid methyl esters. Consequently, the signal at 175.6 ppm is attributed to a carboxylic acid group, while the signal at 172.8 ppm is assigned to carboxyl groups in the form of methyl esters (upfield shifted) (Figures 9-12 and Tables 4, 5) [34-36]. Approximately 70% of the current carboxyl groups are methyl esterified (MeO : ^{13}C , 54.9 ppm; ^1H , 3.85 ppm). The extent of methyl esterification was calculated by comparing the integral intensity of the methyl ester signal (3.85 ppm, 0.5 H) to that of the aliphatic proton signal at H-1 (5.2 ppm, 0.7 H) in a ^1H experiment that included a WATERGATE water suppression routine. The presence of methoxy groups at C3'' and C4'' in the aromatic ring is excluded, as there are no downfield shifts of the C 3'' (145.3 ppm) and C 4'' (144.5 ppm) signals, which could result from substituting the C3'' and C4'' hydroxy groups with methyl groups.

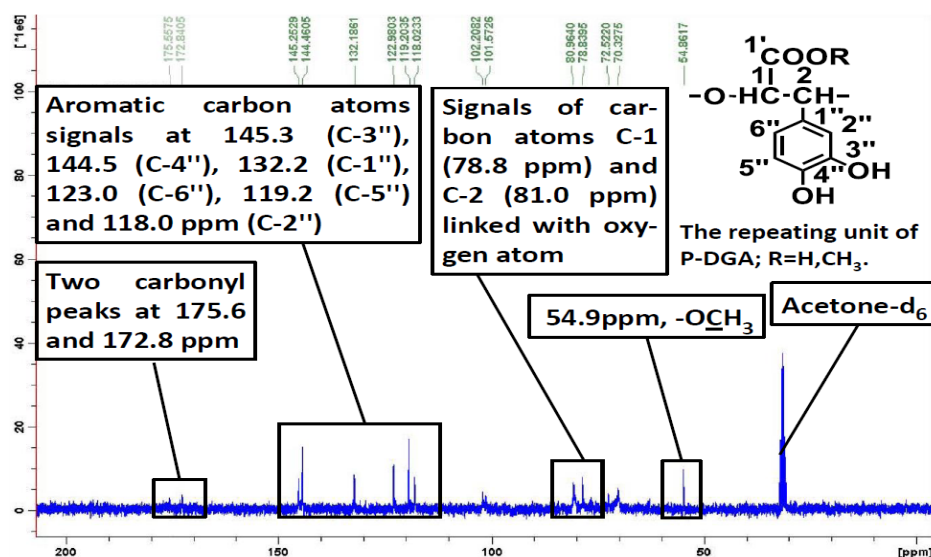


Figure 9. The ^{13}C NMR spectrum of P-DGA from AI, SG, and BO was recorded at 80 °C.

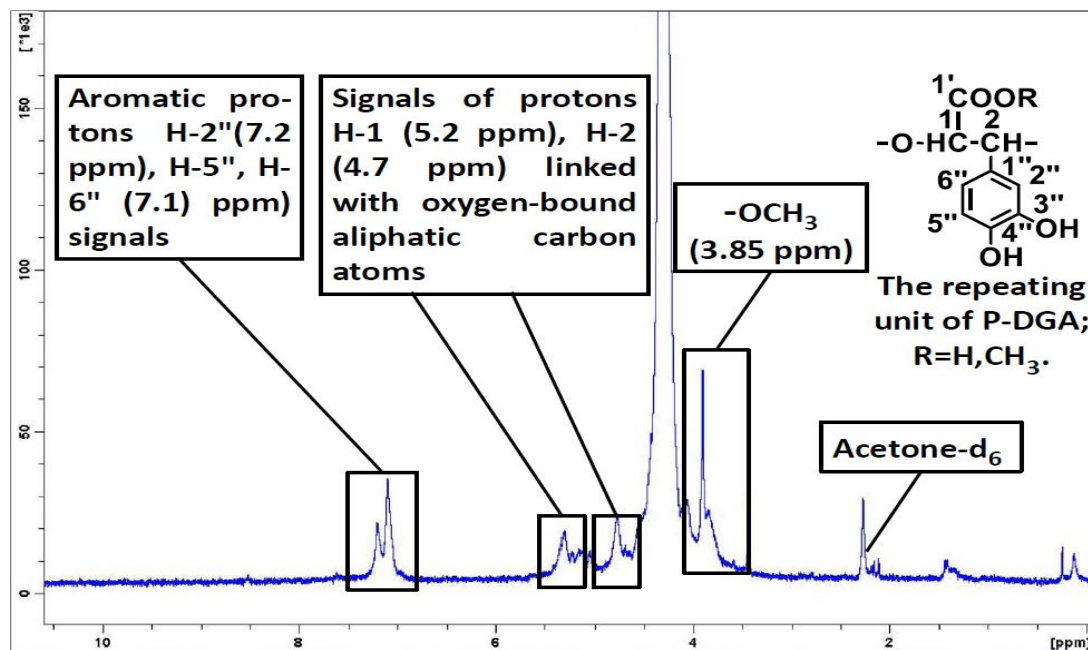


Figure 10. The ¹H NMR spectrum of P-DGA from AI, SG, and BO at 80 °C.

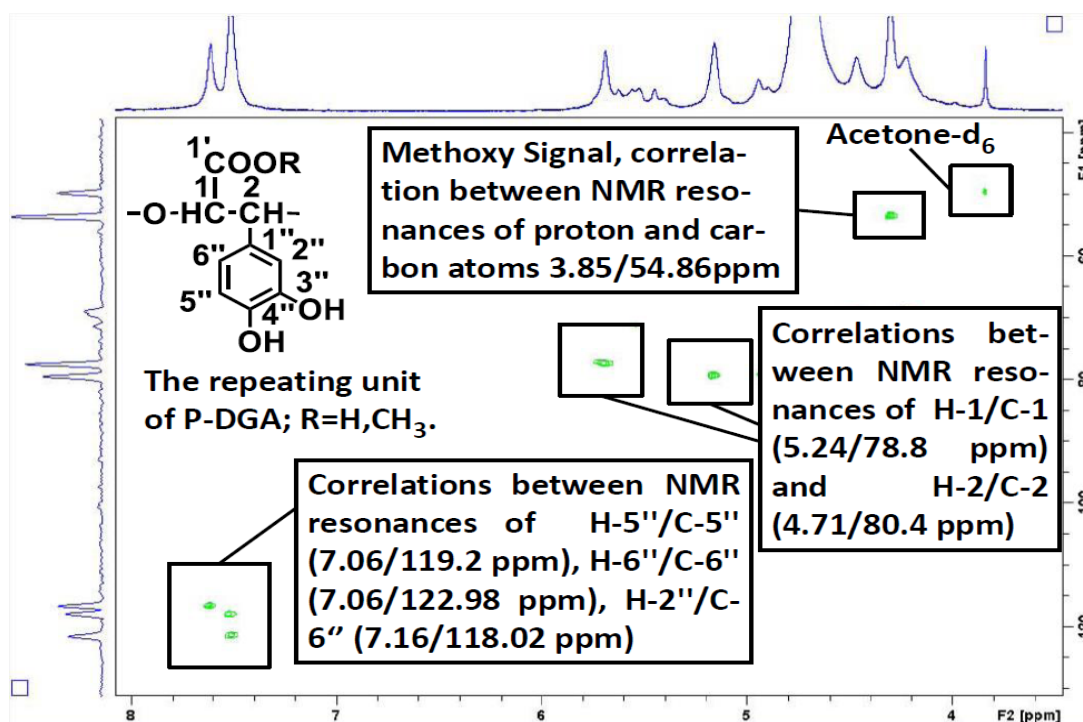


Figure 11. The 2D ¹H/¹³C gHSQCED spectrum of P-DGA from AI, SG, and BO at 80 °C.

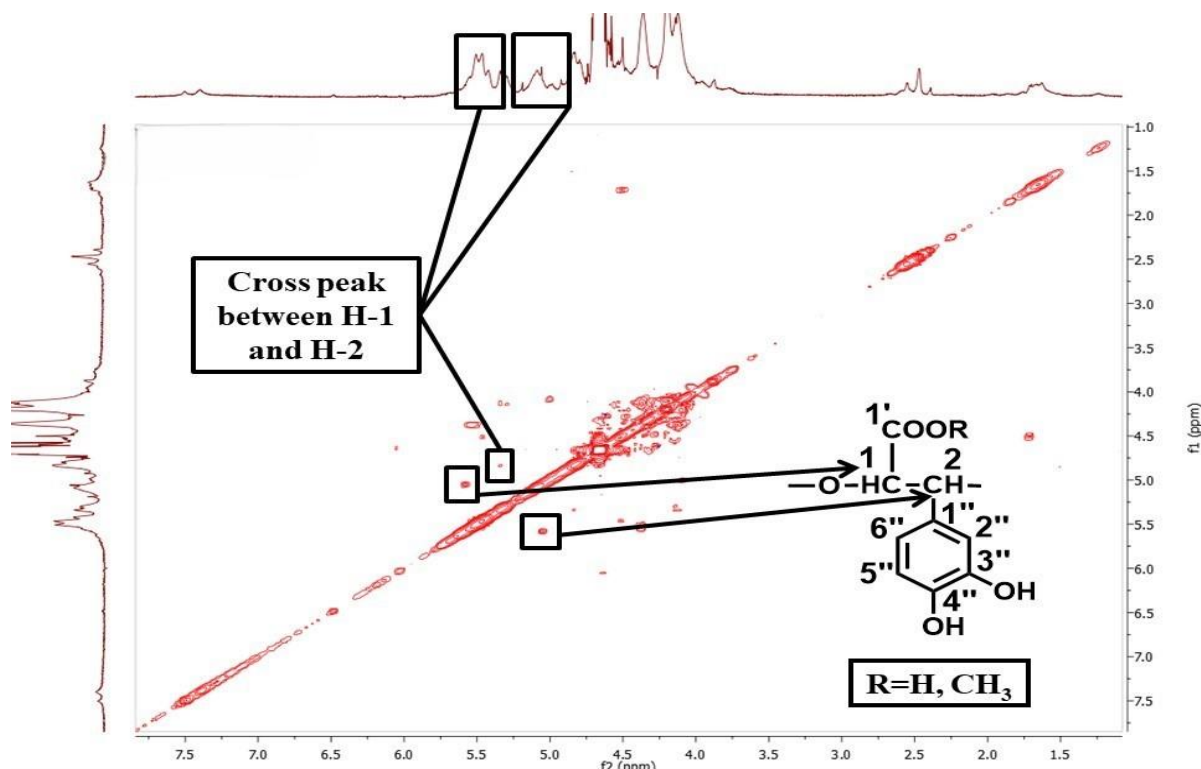


Figure 12. The 2D COSY spectrum of P-DGA from AI, SG, and BO at 80 °C.

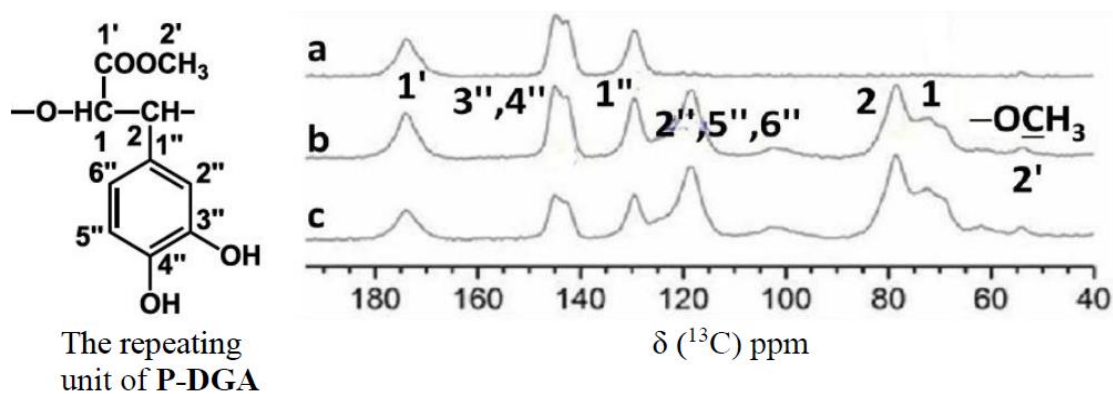
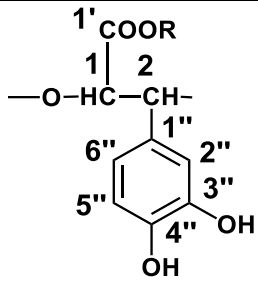


Figure 13. Solid-state $^{13}\text{C}\{^1\text{H}\}$ CP/MAS NMR spectrum of methylated carboxylic groups in P-DGA of SG. a) The spectrum is recorded using a 67.0 microseconds (μs) dipolar dephasing filter and a cross-polarization (CP) time of 3.0 milliseconds (ms); b) The spectrum is recorded with a CP time of 3.0 ms; c) The spectrum is recorded with a CP time of 1.0 ms.

Table 4. The signal assignments of the ^{13}C and ^1H NMR spectra of methylated carboxylic groups in P-DGA (δ_{C} , ppm) from AI, SG, and BO.

The repeating unit of P-DGA; R=H, CH ₃	C atom no.	^{13}C chemical shift, δ_{C} , ppm	^1H chemical shift, δ_{H} , ppm
	1'	175.6 ($-\text{COOH}$)	
	1'	172.8 ($-\text{COOCH}_3$)	3.85
		54.9 ($-\text{OCH}_3$)	($-\text{OCH}_3$)
	1	78.8	5.2
	2	81.0	4.7
	1''	132.2	
	2''	118.0	7.2
	3''	145.3	
	4''	144.5	
	5''	119.2	7.1
	6''	123.0	7.1

Furthermore, the 2D DOSY experiment produced similar diffusion coefficients for both the methylated and non-methylated signals. Both sets of signals occupied the same horizontal range (**Figure 14**). This indicates a comparable molecular weight (same order of magnitude) for methylated and non-methylated polymers [36–38]. This was further supported by graphical representations of the intensity decay of the ^1H signals from aromatic H-2 and aliphatic H-1 at 7.2 and 5.2 ppm (**Figures 15a** and **15b**, respectively), as well as from the methoxy group at 3.85 ppm (**Figure 15c**). These three ^1H signals exhibited essentially the same curve shape. In contrast, the resonance from residual water at 4.35 ppm (**Figure 15d**) displayed a different decay pattern (faster diffusion) (**Figure 15**) [34–36].

Table 5. The signal assignments of the solid-state $^{13}\text{C}\{^1\text{H}\}$ CP/MAS NMR spectrum for methylated carboxylic groups of **P-DGA** (δ_{C} , ppm) from SG.

C atom no.	^{13}C chemical shift, δ_{C} , ppm
1	72
2	78
1'	174
2' ($-\text{OCH}_3$)	54
1''	130
2'',5'',6''	118
3'',4''	143

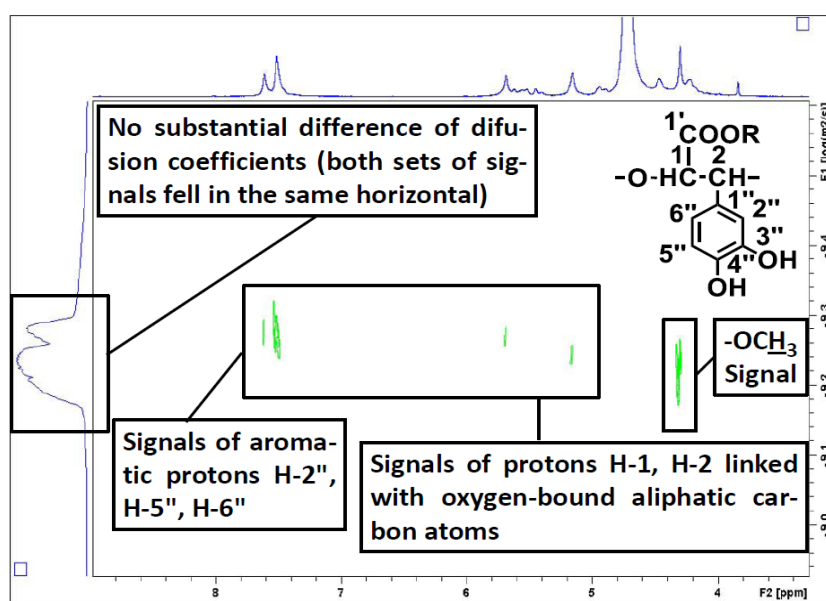


Figure 14. The 2D DOSY experiment of **P-DGA** from **AI** was conducted at 80 °C.

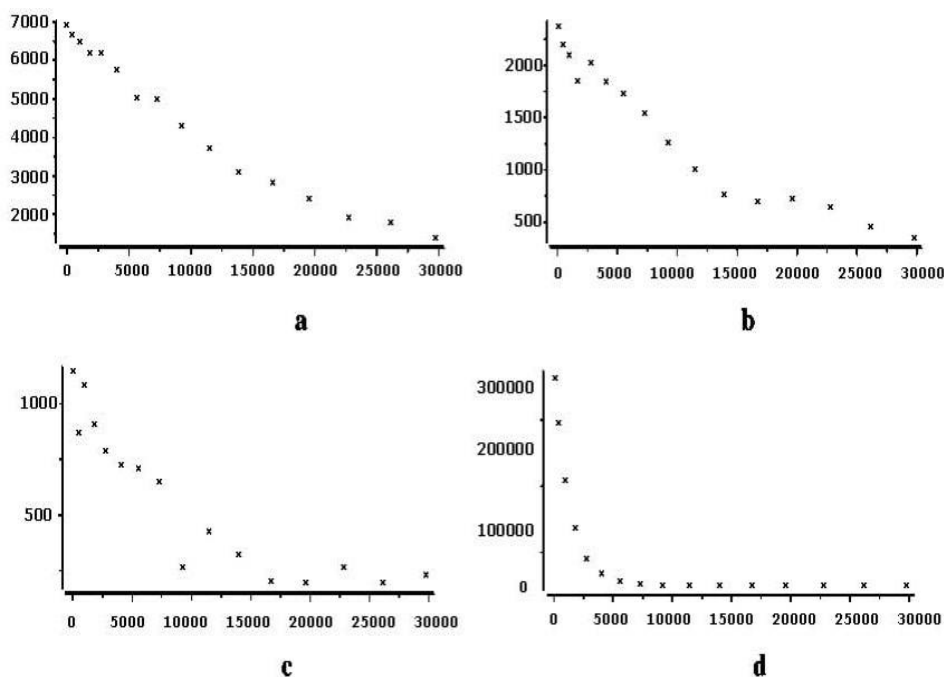


Figure 15. Intensity decay of ^1H signals at 7.2 ppm (Ar H-2") (a), 5.2 ppm (H-1) (b), 3.85 ppm (OMe) (c), and 4.35 ppm (residual water) (d). Units: X-axis in s/cm²; Y-axis in relative intensity (dimensionless).

Thus, based on the data regarding the various techniques of NMR spectroscopy, the main structural component of **HMPs** isolated from **AI**, **SG**, and **BO** is similar to that from **SA**, **SC**, **SO**, **CO**, and **PI** — regular poly[3-(3,4-dihydroxyphenyl)glyceric acid] (**P-DGA**), with a 3-(3,4-dihydroxyphenyl)glyceric acid residue serving as the repeating unit (Figures 1-6, 8-13 and Tables 1-5). However, most of the carboxylic groups in the **P-DGA** from **AI**, **SG**, and **BO** are methylated, unlike those in **P-DGA** from **SA**, **SC**, **SO**, **CO**, and **PI** (Figures 9-14 and Tables 4, 5).

It is important to emphasize that **P-DGA** was detected in neither the leaves of **SA**, **SC**, **SO**, **CO**, **AI**, **SG**, **BO**, and **PI** [27-36, 44] nor in the stems of **AI** [34].

2.3. Proposing Multiple Hydrogen Bonds between **P-DGA** and the Residual Polysaccharides Leads to Supramolecular Association, Resulting in a Multiple-hydrogen-bonded Supramolecular Polymer

We could not fully achieve the separation of **P-DGA** and residual polysaccharides through ultrafiltration. On the one hand, this suggests that **P-DGA** and the residual polysaccharides have similar molecular masses, being of the same order of magnitude. On the other hand, this is likely due to the formation of multiple hydrogen bonds between **P-DGA** and the residual polysaccharides, resulting in a supramolecular associate (multiple-hydrogen-bonded supramolecular polymer). Additionally, **P-DGA** was subjected to gel chromatography on the Sepharose 2B column. The anticomplementary activity by the alternative pathway (AP) eluted together with the UV-286 nm absorption pattern, indicating that it coincided with **P-DGA** but does not align with the carbohydrate's elution curve. The elution peak of the polysaccharides has shifted away from the AP and **P-DGA** peaks. Thus, this phenomenon presumably excludes the covalent binding of residual polysaccharides to **P-DGA**, which is responsible for the anticomplementary activity [20, 31].

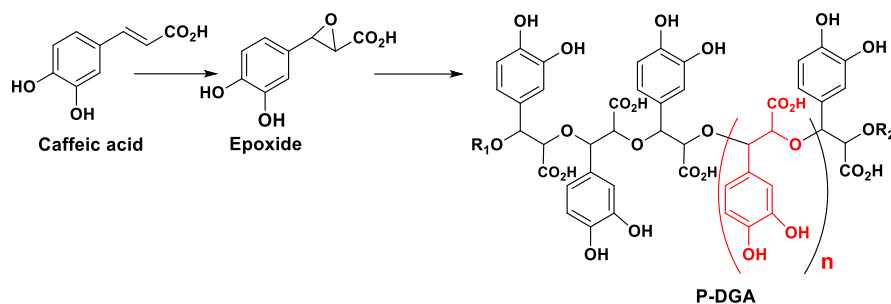
Biopolymers are often impure. They may bind to polysaccharides, proteins, phenolics, etc., substances through either covalent or non-covalent bonds. When highly directional non-covalent interactions replace the covalent bonds that hold the monomeric units of a macromolecule together, supramolecular polymers are formed. Supramolecular chemistry, also referred to as "chemistry beyond the molecule", studies the function and structure of supramolecular entities, i.e., supermolecules arising from the intermolecular binding. Combining supramolecular chemistry and polymer science has given rise to a promising class of nanomaterials called supramolecular polymers. Unlike classical (covalent) polymers, supramolecular polymers are ordered self-assembled nanostructures formed by non-covalent bridging of monomeric units. The diverse applications of supramolecular polymers range from electronics to medicine. The use of supramolecular polymers for intracellular protein delivery, bone regeneration scaffolds, and drug delivery, among other biomedical therapies, is attributed to their versatility and the ability to modulate their physical and mechanical properties. Notably, the application of supramolecular amphiphilic scaffolds in regenerative medicine reveals the promising biomedical applications of these well-ordered systems [45, 46]. This new generation of biopolymers is created through non-covalent interactions such as hydrogen bonding, hydrophobic interactions, π - π electron stacking through the aromatic (arene-arene, $\text{Ar}\cdots\text{Ar}$) structures, π - π electron stacking of aromatic-carbonyl (arene-carbonyl, $\text{Ar}\cdots\text{C}=\text{O}$) structures, π - π electron stacking of carbonyl-carbonyl ($\text{C}=\text{O}\cdots\text{C}=\text{O}$) structures, cation- π interactions, coordination with metal oxide surfaces, and with metal ions to form supramolecular polymers [47, 48].

Catechol, the *ortho* isomer of 1,2-dihydroxybenzene, can bind to mucins by forming hydrogen bonds due to the hydroxyl groups at the *ortho* position. A significant advantage of catechol is its availability for conjugation with bioactive molecules; it can be easily oxidized to the quinone form, which is highly reactive toward numerous functional groups, including thiol and amino groups, via Michael addition or Schiff base reactions. Catechol moieties are suitable for conjugation with metals and metal oxides (i.e., Ag^+ , Fe^{3+} , etc.) through coordination bonds. Furthermore, the unique combination of hydroxyl and phenolic groups can promote π - π stacking and π -cation interactions [48].

Thus, according to the literature data, the two hydroxyl groups of the catechol moieties of **P-DGA** can form hydrogen bonds with the hydroxyl groups of residual polysaccharides. Proposing multiple hydrogen bonds between **P-DGA** and the residual polysaccharides leads to a supramolecular association, resulting in a multiple-hydrogen-bonded supramolecular polymer.

2.4. Proposed Biosynthetic Pathway and Acid Hydrolysis of P-DGA

No information on the biosynthesis of such a polymer in plants is available. However, from the chemical perspective, this process can be viewed as the epoxidation of the double bond in caffeic acid, followed by the polymerization of the resulting epoxide (**Scheme 2**) [28, 29].



Scheme 2. Proposed biosynthetic pathway of **P-DGA**.

Acid hydrolysis (2M CF_3COOH at 121°C for 2 h) of **P-DGA** produced a dark brown or black water-insoluble material. This phenomenon can be explained by the formation of a three-dimensional “lignin-like” compound due to the intermolecular oxidative cross-linking (coupling) between catechol moieties in different macromolecules of [20].

Further research should clarify the physiological functions of these polyethers in plants and demonstrate whether their biosynthesis is a unique characteristic of the Boraginaceae family or if such compounds are also produced in other plants [28, 29].

3. Conclusion

The bioactivity-guided fractionation of water-soluble high-molecular preparations (**HMPs**) from Boraginaceae species — *Symphytum asperum*, *S. caucasicum*, *S. officinale*, *S. grandiflorum*, *Anchusa italica*, *Cynoglossum officinale*, *Borago officinalis*, and *Paracynoglossum imeretinum* — revealed that the key constituent of these **HMPs** is the inaugural representative of a novel class of natural polyethers: poly[oxy-1-carboxy-2-(3,4-dihydroxyphenyl)ethylene], known as poly[3-(3,4-dihydroxyphenyl)glyceric acid] (**P-DGA**). The **PEG** chain serves as the backbone of this biopolymer, with a residue of 3-(3,4-dihydroxyphenyl)glyceric acid acting as the repeating unit. The 3,4-dihydroxyphenyl (catechol) and carboxyl groups regularly substitute for two carbon atoms in the chain. The structure of **P-DGA** was elucidated using data from various NMR techniques, including liquid-state ^1H and ^{13}C NMR, homonuclear 2D gCOSY, heteronuclear 2D $^1\text{H}/^{13}\text{C}$ gHSQCED, 2D DOSY, and solid-state ^{13}C NMR spectra.

The synergistic combination of catecholic groups with the **PEG** main chain of **P-DGA** highlights the diverse and fascinating biological activity of **P-DGA** [13]. **P-DGA** exhibited immunomodulatory (anticomplementary) [20, 31, 49], antioxidant [20, 22, 29, 49, 50], anti-inflammatory [22, 31, 49], wound and burn healing [51, 52], anticancer [53], and antimicrobial [54] activities. Each repeating structural unit of the regular biopolymer **P-DGA** is tri-functional, comprising two catechol *vicinal* hydroxyl groups and one carboxyl group, likely responsible for its broad spectrum of biological activities. Incorporating catechol moieties into macromolecules enhances the exceptional therapeutic properties [10, 12, 55–57]. Conversely, the polymeric component — the **PEG** backbone — of **P-DGA** protects catecholic moieties from rapid degradation and ensures sustained biological efficacy. Consequently, pyrrolizidine alkaloid-free preparations of **P-DGA** may hold potential pharmaceutical value and are recommended for external and internal medical applications.

4. The Future-directed Plan

In the future, we plan to conduct the next review, which will present a detailed description of the biological activities and the structure-bioactivity relationship of **P-DGA** based on the literature data concerning catechol-derived natural and synthetic polymers.

Abbreviations

The following abbreviations are used in this manuscript:

AI	<i>Anchusa italica</i>
APT	Attached proton test
BO	<i>Borago officinale</i>
CO	<i>Cynoglossum officinale</i>
CP	Cross-polarization
CP/MAS	Cross-polarization/magic-angle spinning
DOSY	Diffusion-ordered spectroscopy
gCOSY	Gradient-Selected Correlation Spectroscopy
gHSQCED	Gradient Heteronuclear Single Quantum Coherence and Double Exclusion
HMPs	High-molecular-weight preparations
IR	Infrared
kDa	Kilodalton
NMR	Nuclear magnetic resonance
P-DGA	Poly[3-(3,4-dihydroxyphenyl)glyceric acid]
PEG	Polyethylene glycol
PI	<i>Paracynoglossum imeretinum</i>
ppm	Parts per million
SA	<i>Symphytum asperum</i>
SC	<i>Symphytum caucasicum</i>
SG	<i>Symphytum grandiflorum</i>
SO	<i>Symphytum officinale</i>
UF	Ultrafiltration
UV	Ultraviolet

Conflicts of Interest: The authors declare no conflicts of interest.

References

1. Folashade, K.O.; Omoregie, E.H.; Ochogu, A.P. Standardization of herbal medicines. *Intern. J. Biodiversity Conserv.* 2012, 4 (3), 101–112. <https://doi.org/10.5897/IJBC11.163>
2. Wang, H.; Chen, Y.; Wang, L.; Liu, Q. et al. Advancing herbal medicine: enhancing product quality and safety through robust quality control practices. *Front. Pharmacol.* 2023, 14, 1265178. <https://doi.org/10.3389/fphar.2023.1265178>
3. Chaachouay, N.; Zidane, L. Plant-Derived Natural Products: A Source for Drug Discovery and Development. *Drugs Drug Candidates* 2024, 3, 184–207. <https://doi.org/10.3390/ddc3010011>
4. Umadevi, M.; Kumar, K.P.S.; Bhowmik, D.; Duraivel, S. Traditionally Used Anticancer Herbs in India. *J. Med. Plants Studies* 2013, 1 (3), 56–74. <https://www.plantsjournal.com/archives/2013/vol1issue3/PartA/6-378.pdf>
5. Vaou, N.; Stavropoulou, E.; Voidarou, C.; Tsakris, Z. et al. Interactions between Medical Plant-Derived Bioactive Compounds: Focus on Antimicrobial Combination Effects. *Antibiotics* 2022, 11 (8), 1014 (1–23). <https://doi.org/10.3390/antibiotics11081014>
6. Muscolo, A.; Mariateresa, O.; Giulio, T.; Mariateresa, R. Oxidative Stress: The Role of Antioxidant Phytochemicals in the Prevention and Treatment of Diseases. *Int. J. Mol. Sci.* 2024, 25 (6), 3264 (1–22). <https://doi.org/10.3390/ijms25063264>
7. Qureshi, D.; Nayak, S.K.; Anis, A.; Ray, S.S. et al. Chapter 1 – Introduction of biopolymers: Food and biomedical applications. In *Biopolymer-Based Formulations. Biomedical and Food Applications*; Pal, K.; Banerjee, I.; Sarkar, P.; Kim, D.; Deng, W.-P.; Dubey, N.K.; Majumder, K., Eds.; Elsevier Inc.: Amsterdam, Netherlands, 2020; pp. 1–45. <https://doi.org/10.1016/B978-0-12-816897-4.00001-1>
8. Al-Ghraibah, A.M.; Al-Qudah, M.; AL-Oqla, F.M. Chapter 10 - Medical Implementations of Biopolymers. In *Advanced Processing, Properties, and Applications of Starch and Other Bio-Based Polymers*; Al-Oqla, F.M.; Sapuan, S.M., Eds.; Elsevier Inc.: Amsterdam, Netherlands, 2020; pp. 157–171. <https://doi.org/10.1016/B978-0-12-819661-8.00010-X>
9. Nitta, S.K.; Numata, K. Biopolymer-Based Nanoparticles for Drug/Gene Delivery and Tissue Engineering. *Int. J. Mol. Sci.* 2013, 14 (1), 1629–1654. <https://doi.org/10.3390/ijms14011629>
10. Nishimoto-Sauceda, D.; Romero-Robles, L.E.; Antunes-Ricardo, M. Biopolymer nanoparticles: a strategy to enhance stability, bioavailability, and biological effects of phenolic compounds as functional ingredients. *J. Sci. Food Agric.* 2022, 102 (1), 41–52. <https://doi.org/10.1002/jsfa.11512>
11. Nemli, E.; Ozkan, G.; Subasi, B.G.; Cavdar, H. et al. Interactions between proteins and phenolics: effects of food processing on the content and digestibility of phenolic compounds. *J. Sci. Food Agric.* 2024, 104, 2535–2550. <https://doi.org/10.1002/jsfa.13275>
12. Foujdar, R.; Bera, M.B.; Chopra, H.K. Chapter 30 - Phenolic nanoconjugates and their application in food. In *Biopolymer-Based Formulations. Biomedical and Food Applications*; Pal, K.; Banerjee, I.; Sarkar, P.; Kim, D.; Deng, W.-P.; Dubey, N.K.; Majumder, K., Eds.; Elsevier Inc.: Amsterdam, Netherlands, 2020; pp. 751–780. <https://doi.org/10.1016/B978-0-12-816897-4.00030-8>

13. Patil, N.; Jérôme, C.; Detrembleur, C. Recent Advances in the Synthesis of Catechol-Derived (Bio)Polymers for Applications in Energy Storage and Environment. *Prog. Polym. Sci.* 2018, 8, 34–91. <https://doi.org/10.1016/j.progpolymsci.2018.04.002>
14. Mashhadi, S.M.A.; Yufit, D.; Liu, H.; Hodgkinson, P. et al. Synthesis and structural characterization of cocrystals of isoniazid and cinnamic acid derivatives. *J. Mol. Struct.* 2020, 1219 (24), 128621 (1–20). <https://doi.org/10.1016/j.molstruc.2020.128621>
15. Dresler, S.; Szymczak, G.; Wojcik, M. Comparison of some secondary metabolite content in the seventeen species of the Boraginaceae family. *Pharm. Biol.* 2017, 55 (1), 691–695. <http://dx.doi.org/10.1080/13880209.2016.1265986>
16. Taravati, G.; Masoudian, N.; Gholamian, A. Evaluation of Medical Metabolites in Boraginaceae Family. *J. Chem. Health Risks* 2014, 4 (1), 53–61. <https://www.jchr.org/index.php/JCHR/article/view/391/393>
17. Gupta, P.S.P.; Vishwakarma, K.; Soni, P.; Jadhao, A.B. et al. Medicinally Important Plants of Boraginaceae Family. *Afr. J. Bio. Sc.* 2024, 6 (Si4), 6013–6021. <https://doi.org/10.48047/Afjbs.6.Si4.2024.6013-6021>
18. Dominguez de Maria, P.; van Gemert, R.W.; Straathof, A.J.J.; Hanefeld, U. Biosynthesis of ethers: Unusual or common natural events? *Nat. Prod. Rep.* 2010, 27, 370–392. <https://doi.org/10.1039/b809416k>
19. Hatfield, W.; Vermerris, W. Lignin formation in plants. The dilemma of linkage specificity. *Plant Physiol.* 2001, 126 (4), 1351–1357. <https://doi.org/10.1104/pp.126.4.1351>
20. Barbakadze, V.; Kemertelidze, E.; Usov, A.I.; Kroes, B.H. et al. Evaluation of immunomodulatory activity of some plant polysaccharides. *Proc. Georgian Acad. Sci., Biol. Ser.* 1999, 25 (4–6), 207–216. https://www.researchgate.net/publication/285495080_Evaluation_of_immunomodulatory_activity_of_some_plant_polysaccharides
21. Tsuda, Y. Isolation of Natural Products; Japan Analytical Industry Co., Ltd.: Tokyo, Japan, 2004; p. 40. http://natpro.com.vn/public/assets/Download/Isolation_of_Natural_Products.pdf
22. Barthomeuf, C.M.; Debiton, E.; Barbakadze, V.V.; Kemertelidze, E.P. Evaluation of the dietetic and therapeutic potential of a high molecular weight hydroxycinnamate-derived polymer from *Symphytum asperum* Lepech. *J. Agric. Food Chem.* 2001, 49 (8), 3942–3946. <https://doi.org/10.1021/jf010189d>
23. Gogilashvili, L.; Amiranashvili, L.; Barbakadze, V.; Merlani, M. et al. Obtaining of toxic pyrrolizidine alkaloid-free biologically active high molecular preparations of *Symphytum asperum* and *S. caucasicum*. *Bull. Georg. Natl. Acad. Sci.* 2008, 2 (2), 85–89. <http://science.org.ge/old/moambe/2-2/Gogilashvili.pdf>
24. Barbakadze, V.V.; Kemertelidze, E.P.; Dekanosidze, H.E.; Beruchashvili, T.G.; Usov, A.I. Investigation of Glucofructans from Roots of Two Species of Comfrey *Symphytum asperum* Lepech. and *S. caucasicum* Bieb. *Rus. J. Bioorg. Chem.* 1992, 18 (5), 671–679 (in Russian). #abstract in English. <https://eurekamag.com/research/007/485/007485437.php>
25. Gallastegui, A.; Camara, O.; Minudri, D.; Goujon, N. et al. Aging Effect of Catechol Redox Polymer Nanoparticles for Hybrid Supercapacitors. *Batteries&Supercaps* 2022, 5 (9), e202200155 (1–9). <https://doi.org/10.1002/batt.202200155>

26. Dyer, M.A. Applications of Absorption Spectroscopy of Organic Compounds; Prentice-Hall Inc.: Englewood Cliffs, NY, USA, 1965.
27. Barbakadze, V.V.; Kemertelidze, E.P.; Shashkov, A.S.; Usov, A.I. Structure of a new anticomplementary dihydroxycinnamate-derived polymer from *Symphytum asperum* (Boraginaceae). Mendeleev Commun. 2000, 10 (4), 148–149.
<https://doi.org/10.1070/MC2000v010n04ABEH001295>
28. Barbakadze, V.V.; Kemertelidze, E.P.; Targamadze, I.L.; Shashkov, A.S.; Usov, A.I. Poly[3-(3,4-Dihydroxyphenyl)glyceric Acid]: A New Biologically Active Polymer from Two Comfrey Species *Symphytum asperum* and *S. caucasicum* (Boraginaceae). Rus. J. Bioorg. Chem. 2002, 28 (4), 326–330.
<https://doi.org/10.1023/A:1019552110312>
29. Barbakadze, V.; Kemertelidze, E.; Targamadze, I.; Mulkijanyan, K. et al. Poly[3-(3,4-dihydroxyphenyl)glyceric Acid], A New Biologically Active Polymer from *Symphytum asperum* Lepech. and *S. caucasicum* Bieb. (Boraginaceae). Molecules 2005, 10 (9), 1135–1144.
<https://doi.org/10.3390/10091135>
30. Barbakadze, V.V.; Kemertelidze, E.P.; Targamadze, I.; Mulkidzhanyan, K. et al. Poly[3-(3,4-dihydroxyphenyl)glyceric acid] from Stems of *Symphytum asperum* and *S. caucasicum*. Chem. Nat. Compd. 2005, 41 (4), 374–377. <https://doi.org/10.1007/s10600-005-0155-2>
An erratum to this article: Chem. Nat. Compd., 2005, 41 (5), 615. <http://dx.doi.org/10.1007/s10600-005-0226-4>
31. Barbakadze, V.; van den Berg, A.J.J.; Beukelman, C.J.; Kemmink, J. et al. Poly[3-(3,4-dihydroxyphenyl)glyceric acid] from *Symphytum officinale* roots and its biological activity. Chem. Nat. Compd. 2009, 45 (1), 6–10. <https://doi.org/10.1007/s10600-009-9221-5>
32. Gogilashvili, L.; Amiranashvili, L.; Salgado, A.; Barbakadze, V. et al. Poly[3-(3,4-Dihydroxyphenyl)Glyceric Acid] from *Cynoglossum officinale* L. (Boraginaceae). Bull. Georg. Natl. Acad. Sci. 2020, 14 (1), 108–113.
http://science.org.ge/bnas/t14-n1/16_Gogilashvili_Pharmacochemistry.pdf
33. Barbakadze, V.; Gogilashvili, L.; Amiranashvili, L.; Merlani, M. et al. Biologically Active Sugar-Based Biopolyether Poly[3-(3,4-Dihydroxyphenyl)Glyceric Acid] from the Stems and Roots of *Paracynoglossum imeretinum* (Kusn.) M.Pop. Bull. Georg. Natl. Acad. Sci. 2022, 16 (3), 110–115.
<http://science.org.ge/bnas/vol-16-3.html>
34. Barbakadze, V.; Gogilashvili, L.; Amiranashvili, L.; Merlani, M. et al. Poly[3-(3,4-dihydroxyphenyl)glyceric Acid] from *Anchusa italica* Roots. Nat. Prod. Commun. 2010, 5 (7), 1091–1095.
<https://doi.org/10.1177/1934578X1000500722>
35. Gokadze, S.; Gogilashvili, L.; Amiranashvili, L.; Barbakadze, V. et al. Investigation of Water-Soluble High Molecular Preparation of *Symphytum grandiflorum* DC (Boraginaceae). Bull. Georg. Natl. Acad. Sci. 2017, 11 (1), 116–121. http://science.org.ge/bnas/t11-n1/19_Gokadze.pdf
36. Barbakadze, V.; Gogilashvili, L.; Amiranashvili, L.; Merlani, M. et al. Carbohydrate-Based Biopolymers: Biologically Active Poly[3-(3,4-Dihydroxyphenyl)Glyceric Acid] from *Borago officinalis*. Bull. Georg. Natl. Acad. Sci. 2021, 15 (4), 140–145. <http://science.org.ge/bnas/vol-15-4.html>
37. Patt, S.L.; Schoolery, J.N. Attached proton test for carbon-13 NMR. J. Magn. Reson. 1982, 46 (3), 535–539. [https://doi.org/10.1016/0022-2364\(82\)90105-6](https://doi.org/10.1016/0022-2364(82)90105-6)

38. Pagenkopf, B. ACD/HNMR Predictor and ACD/CNMR Predictor Advanced Chemistry Development, Inc. (Computer Software Review). J. Am. Chem. Soc. 2005, 127 (9), 3232. <https://doi.org/10.1021/ja040946z>
39. Van Bramer, S. ACD/CNMR and ACD/HNMR Spectrum Prediction Software. (Software Review). Conc. Magn. Reson. 1997, 9 (4), 271–273. [https://doi.org/10.1002/\(SICI\)1099-0534\(1997\)9:4<271::AID-CMR6>3.0.CO;2-W](https://doi.org/10.1002/(SICI)1099-0534(1997)9:4<271::AID-CMR6>3.0.CO;2-W)
40. Barbakadze, V.; Kemertelidze, E.; Shashskov, A.S.; Usov, A.I. et al. Partial characterization of a new anticomplementary dihydroxycinnamate-derived polymer from *Symphytum asperum* Lepech. Proc. Georg. Acad. Sci., Biol. Ser. 1999, 25 (4–6), 199–205. https://www.researchgate.net/publication/377261995_Partial_Characterization_Dihydroxycinnamate-derived
41. Lomsadze, K.; Lengers, I.; Barbakadze, V.; Kohler, J. et al. The investigation of structural characteristics of biologically active natural polymers using solid-state NMR experiments. 34th International Symposium on Pharmaceutical and Biomedical Analysis (PBA 2024), Geneva, Switzerland, September 9–12, 2024; pp. 73–74.
42. Mao, J.D.; Schmidt-Rohr, K. Accurate quantification of aromaticity and non-protonated aromatic carbon fraction in natural organic matter by C-13 solid-state nuclear magnetic resonance. Environ. Sci. Technol. 2004, 38 (9), 2680–2684. <https://doi.org/10.1021/es034770x>
43. Freitas, J.C.C.; Ejaz, M.; Toci, A.T.; Romao, W. et al. Solid-state NMR spectroscopy of roasted and ground coffee samples: Evidences for phase heterogeneity and prospects of applications in food screening. Food Chem. 2023, 409, 135317 (1–9). <https://doi.org/10.1016/j.foodchem.2022.135317>
44. Barbakadze, V.V.; Mulkidzhanyan, K.G.; Merlani, M.I.; Gogilashvili, L.M. et al. Extraction, composition, and the antioxidant and anticomplement activities of high molecular weight fractions from the leaves of *Symphytum asperum* and *S. caucasicum*. Pharm. Chem. J. 2011, 44 (11), 604–607. <https://doi.org/10.1007/s11094-011-0527-9>
45. Riseh, R.S.; Hassanisaadi, M.; Vatankhah, M.; Varma, R.S. et al. Nano/Micro-Structural Supramolecular Biopolymers: Innovative Networks with the Boundless Potential in Sustainable Agriculture. Nano-Micro Lett. 2024, 16, 147 (1–23). <https://doi.org/10.1007/s40820-024-01348-x>
46. Martínez-Orts, M.; Pujals, S. Responsive Supramolecular Polymers for Diagnosis and Treatment. Int. J. Mol. Sci. 2024, 25, 4077 (1–27). <https://doi.org/10.3390/ijms25074077>
47. Zhang, W.; Wang, R.; Sun, Z.; Zhu, X. et al. Catechol functionalized hydrogels: Biomimetic design, adhesion mechanism, and biomedical applications. Chem. Soc. Rev. 2020, 49 (2), 433–464. <https://doi.org/10.1039/c9cs00285e>
48. Dubashynskaya, N.V.; Petrova, V.A.; Skorik, Y.A. Biopolymer Drug Delivery Systems for Oromucosal Application: Recent Trends in Pharmaceutical R&D. Int. J. Mol. Sci. 2024, 25 (10), 5359. <https://doi.org/10.3390/ijms25105359>
49. Barbakadze, V.V.; Kemertelidze, E.P.; Mulkijanyan, K.G.; van den Berg, A.J.J. et al. Antioxidant and anticomplement activity of poly[3-(3,4-dihydroxyphenyl)glyceric acid] from *Symphytum asperum* and *Symphytum caucasicum* plants. Pharm. Chem. J. 2007, 41 (1), 14–16. <https://doi.org/10.1007/s11094-007-0004-7>

An erratum to this article: Pharm. Chem. J., 2007, 41 (3), 178. <http://dx.doi.org/10.1007/s11094-007-0040-3>

50. Merlani, M.; Barbakadze, V.; Gogilashvili, L.; Amiranashvili, L. Antioxidant Activity of Caffeic Acid-Derived Polymer from *Anchusa italica*. Bull. Georg. Natl. Acad. Sci. 2017, 11 (2), 123–127. <http://science.org.ge/bnas/vol-11-2.html>
51. Barbakadze, V.; Mulkijanyan, K.; Gogilashvili, L.; Amiranashvili, L. et al. Allantoin- and Pyrrolizidine Alkaloids-Free Wound Healing Compositions from *Symphytum asperum*. Bull. Georg. Natl. Acad. Sci. 2009, 3 (1), 159–164. <http://science.org.ge/old/3-1/Barbakadze.pdf>
52. Mulkijanyan, K.; Barbakadze, V.; Novikova, Zh.; Sulakvelidze, M. et al. Burn Healing Compositions from Caucasian Species of Comfrey (*Symphytum* L.). Bull. Georg. Natl. Acad. Sci. 2009, 3 (3), 114–117. <http://science.org.ge/old/moambe/3-3/Mulkijanian.pdf>
53. Shrotriya, S.; Gagan, D.; Ramasamy, K.; Raina, K. et al. Poly[3-(3,4-dihydroxyphenyl)glyceric acid] from Comfrey exerts anti-cancer efficacy against human prostate cancer via targeting androgen receptors, cell cycle arrest, and apoptosis. Carcinogenesis 2012, 33 (8), 1572–1580. <https://doi.org/10.1093/carcin/bgs202>
54. Barbakadze, V.; Merlani, M.; Gogilashvili, L.; Amiranashvili, L. et al. Antimicrobial Activity of Catechol-Containing Biopolymer Poly[3-(3,4-dihydroxyphenyl)glyceric Acid] from Different Medicinal Plants of Boraginaceae Family. Antibiotics 2023, 12, 285. <https://doi.org/10.3390/antibiotics12020285>
55. Bruckhuisen, J.; Dhont, G.; Roucou, A.; Jabri, A. et al. Intramolecular H-Bond Dynamics of Catechol Investigated by THz High-Resolution Spectroscopy of Its Low-Frequency Modes. Molecules 2021, 26 (12), 3645 (1–20). <https://doi.org/10.3390/molecules26123645>
56. Batey, S.F.D.; Davie, M.J.; Hems, E.S.; Liston, J.D. et al. The catechol moiety of obafluorin is essential for antibacterial activity. RSC Chem. Biol. 2023, 4 (11), 926–941. <https://doi.org/10.1039/d3cb00127j>
57. Puertas-Bartolome, M.K.; Włodarczyk-Biegun, M.K.; del Campo, A.; Vazquez-Lasa, B. et al. Development of bioactive catechol functionalized nanoparticles applicable for 3D bioprinting. Mater. Sci. Eng. C 2021, 131, 112515 (1–14). <https://doi.org/10.1016/j.msec.2021.112515>

**Boraginaceae-ს ოჯახის სხვადასხვა სამკურნალო მცენარის ბიოლოგიურად
აქტიური პოლიეთილენგლიკოლის საფუძველზე მრავალკატექოლშემცველი
ბიოპოლიმერი პოლი[3-(3,4-დიჰიდროქსიფენილ)გლიცერინის მჟავა]**

**ვახტანგ ბარბაქაძე, მაია მერლანი, ლალი გოგილაშვილი, ლელა ამირანაშვილი, კარენ
მულკიჯანიანი**

რეზიუმე: მიღებულია Boraginaceae-ს ოჯახის სხვადასხვა სამკურნალო მცენარედან *Symphytum asperum*-ის, *S. caucasicum*-ის, *S. officinale*-ის, *S. grandiflorum*-ის, *Anchusa italica*-ს, *Cynoglossum officinale*-ს, *Borago officinalis*-ის და *Paracynoglossum imeretinum*-ის წყალში ხსნადი მაღალ მოლეკულური (>1000 kDa ან >500 kDa) პრეპარატები (მმპ). ამ მმპ-ების ძირითადი ქიმიური შემადგენელი ნაწილია ბუნებრივი პოლიეთერების აქამდე უცნობი კლასის პირველი და ერთადერთი წარმომადგენელი - ახალი პოლი[ოქსი-1-კარბოქსი-2-(3,4-დიჰიდროქსიფენილ)ეთილენი], რომელიც ასევე ცნობილია როგორც პოლი[3-(3,4-დიჰიდროქსიფენილ)გლიცერინის მჟავა] (პ-დგმ). პ-დგმ-ს სტრუქტურის გარკვევა განხორციელდა ბირთვული მაგნიტური რეზონანსის (ბმრ) სხვადასხვა ტექნიკის მონაცემების გამოყენებით, მათ შორის თხევად ფაზაში ^1H , ^{13}C ბმრ, ორგანზომილებიანი (2D) ჰომონუკლეარული gCOSY, ორგანზომილებიანი (2D) ჰეტერონუკლეარული $^1\text{H}/^{13}\text{C}$ gHSQCED, ორგანზომილებიანი (2D) DOSY (დიფუზიური ორგანიზებული სპექტროსკოპია) და მყარ ფაზაში ^{13}C ბმრ სპექტრები. პოლიოქსიეთილენის (პოლიეთილენგლიკოლის) (პეგ) ჯაჭვი წარმოადგენს ამ ბიოპოლიმერის ხერხემალს, ხოლო 3-(3,4-დიჰიდროქსიფენილ) გლიცერინის მჟავას ნაშთი ფუნქციონირებს როგორც განმეორებადი ერთეული. 3,4-დიჰიდროქსიფენილის (კატექოლი) და კარბოქსილის ჯგუფები არიან რეგულარული ჩამნაცვლებლები პეგ-ის ჯაჭვში. ამრიგად, პ-დგმ წარმოადგენს ბუნებრივი პოლიეთერების უნიკალურ კლასს. პ-დგმ-ის თითოეული განმეორებადი სამფუნქციური სტრუქტურული ერთეული შეიცავს ორ ფენოლის ჰიდროქსილის ჯგუფს *ერთო* პოზიციაში და ერთ კარბოქსილის ჯგუფს. პ-დგმ-ს მრავალფუნქციურობა, სავარაუდოდ, ხსნის მის ბიოლოგიური აქტიურობის ფართო სპექტრს, მათ შორის ანტიკომპლემენტურ, ანტიოქსიდანტურ, ანთების საწინააღმდეგო, დამწვრობისა და ჭრილობების შეხორცების, ანტიმიკრობულ და კიბოს საწინააღმდეგო თვისებებს.